Journal of proteome research

Article

pubs.acs.org/jpr

The Impact of High-Fat Diet on Metabolism and Immune Defense in Small Intestine Mucosa

Jacek R. Wiśniewski,*[,†] Alexandra Friedrich,[‡] Thorsten Keller,[‡] Matthias Mann,[†] and Hermann Koepsell[‡]

[†]Department of Proteomics and Signal Transduction, Max-Planck-Institute of Biochemistry, 82152 Martinsried, Germany

[‡]Department of Molecular Plant Physiology and Biophysics, Julius-von-Sachs-Institute, University of Würzburg, 97082 Würzburg, Germany

Supporting Information

ABSTRACT: Improved procedures for sample preparation and proteomic data analysis allowed us to identify 7700 different proteins in mouse small intestinal mucosa and calculate the concentrations of >5000 proteins. We compared protein concentrations of small intestinal mucosa from mice that were fed for two months with normal diet (ND) containing 34.4% carbohydrates, 19.6% protein, and 3.3% fat or high-fat diet (HFD) containing 25.3% carbohydrates, 24.1% protein, and 34.6% fat. Eleven percent of the quantified proteins were significantly different between ND and HFD. After HFD, we observed an elevation of proteins involved in protein synthesis, protein *N*-glycosylation, and vesicle trafficking. Proteins engaged in fatty acid absorption, fatty acid β-oxidation, and steroid metabolism were also increased. Enzymes of glycolysis and pentose phosphate cycle were decreased, whereas proteins of the respiratory chain and of ATP synthase were increased. The protein concentrations of various nutrient transporters located in the enterocyte plasma membrane including the Na^+-D-glucose cotransporter SGLT1, the passive glucose transporter GLUT2, and the H^+-peptide cotransporter PEPT1 were decreased. The concentration of the Na^+,K^+-ATPase, which turned out to be the most strongly expressed enterocyte transporter, was also decreased. HFD also induced concentration changes of drug transporters and of enzymes involved in drug metabolism, which suggests effects of HFD on pharmacokinetics and toxicities. Finally, we observed down-regulation of antibody subunits and of components of the major histocompatibility complex II that may reflect impaired immune defense and immune tolerance in HFD. Our work shows dramatic changes in functional proteins of small intestine mucosa upon excessive fat consumption.

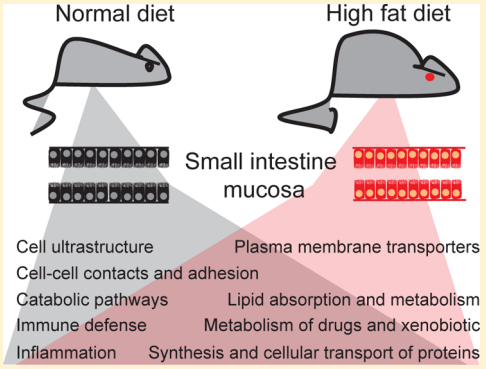

KEYWORDS: *Small intestine, intestinal epithelium, proteomics, nutrition, high-fat diet, intestinal metabolism, nutrient transport, drug transport, immune defense, major histocompatibility complex (MHC)*

INTRODUCTION

The small intestine of mammalians provides an extensive contact surface for ingested compounds that allows the absorption and metabolism of nutrients, xenobiotics, and drugs as well as immune defense against antigenic food components, bacterial and viral pathogens, and immune response to allergens. The performance of these different functions is enabled by unique morphological and functional properties of small intestine. Thus, rapid absorption of hydrophilic compounds is allowed by an extended luminal plasma membrane surface containing many different transporter proteins, by metabolic enzymes within the enterocytes and by transporters within the basolateral membrane (BLM). The extended luminal surface of the small intestine is formed by villi and crypts, which are covered mostly with enterocytes but also contain some additional cells such as secretory cells or lymphocytes. The luminal surface of the enterocytes forms microvilli that lead to a dramatic enlargement. Passive permeation of hydrophilic compounds is prevented by tight junctions between the enterocytes. The soft connective tissue below the enterocytes called lamina propria contains permeable blood vessels that provide removal of absorbed compounds and various immune cells. The enterocytes have a rapid turnover, which allows quick replacement of cells and quick cellular adaptations in response to diets or expose to xenobiotics and pathogens. Previous investigations showed that small intestinal enterocytes contain a large variety of plasma membrane transporters, metabolic enzymes, regulatory proteins, intracellular binding proteins, antibodies, and others;[1−3] however, a comprehensive map of proteins expressed in small intestinal enterocytes is missing.

McCornell et al. identified 646 proteins in a preparation that was isolated from mouse small intestine trying to enrich the brush-border membranes of the enterocytes.[4] The proteins identified in this preparation consisted of cytoskeletal proteins

Special Issue: Environmental Impact on Health

Received: August 8, 2014
Published: October 6, 2014

   dx.doi.org/10.1021/pr500833v | *J. Proteome Res.* 2015, 14, 353−365

(44%), hydrolases (16%), transporters and channels (9%), mitochondrial proteins (9%), nuclear proteins (6%), metabolic enzymes (5%), and others, which indicates a heterogeneous preparation. A similar heterogeneous composition of enterocyte proteins was described using a different procedure trying to purify brush-border membrane (BBM) vesicles.[5]

In our study, we performed an in-depth proteomic analysis of homogenized mucosa that was scraped from everted mice small intestines. This preparation contained enterocytes and some components of the underlying soft connective tissue. By using previously developed procedures for sample preparation and proteomic data analysis,[6−8] we were able to identify 7700 proteins and calculate absolute concentrations of more than 5000 of these proteins, including 88 different plasma membrane transporters. By trying to apply this powerful approach to a biomedical important question, we investigated whether the protein concentrations in the mucosa were different when the mice were kept for two months on a Western-type hypercaloric high-fat diet (HFD) compared to a standard diet. Significant changes with impact on nutrient transport, energetic metabolism, drug transport, drug metabolism, immune defense, and susceptibility to inflammation were observed.

EXPERIMENTAL PROCEDURES

Animals

After male Balb C57BL/6 mice were weaned, they were fed for two months with a normal diet (ND) containing 12.8 MJ/kg metabolizable energy (Ssniff V1534−000R/M) or with a high-fat diet (HFD) containing 25.2 MJ/kg metabolizable energy (Ssniff D12492R/M). The diets were obtained from Spezialdiäten GmbH (Soest, Germany). The animals were housed in a temperature-controlled environment with a 12 h light/12 h dark cycle. They had free access to food and water.

Isolation and Lysis of the Luminal Layer of Small Intestinal Mucosa

Mice were starved overnight and sacrificed in the morning. Directly after killing, the jejunum was removed, everted, and washed with ice-cold phosphate buffered saline (PBS). The luminal layer of the mucosa was removed by gentle scraping with a glass plate, and the obtained material was lysed in 60 mM tris(hydroxymethyl)aminomethane (Tris) HCl, pH 6.8 containing 2% (w/v) sodium dodecyl sulfate (SDS), 100 mM dithiothreitol 7% (v/v) glycerol, and various protease inhibitors. The samples named whole cell lysates (WCLs) were frozen in liquid nitrogen.

Isolation of a Plasma Membrane Enriched Membrane Fraction

To isolate a membrane fraction in which the glycocalix containing BBMs of the enterocytes, we incubated the mucosal scrapings for 30 min at 4 °C in 2-morpholinoethanesulfonate (MES) buffer (20 mM MES, pH 6.0, 80 mM NaCl) containing 1% (w/v) colloidal silica (Ludox Cl, Sigma). After the reaction of silica with the glycocalix 0.1% poly(acrylic acid) was blocked, we homogenized the sample by sonification on ice and removed cell debris, intact nuclei, and intact mitochondria by repeated centrifugation at 1000 × *g* and 10 000 × *g*. In a last step, membranes were spun down by a 60 min centrifugation at 100 000 × *g* (4 °C). The resulting pellet was lysed in SDS (membrane lysate (ML)) and stored as described for the scraped mucosa.

Protein Digestion and Peptide Fractionation

The SDS lysates of whole cells and enriched plasma membrane fractions were processed in 30k filtration units (Cat No. MRCF0R030, Millipore)[9] using the multienzyme digestion (MED)-filter aided sample preparation (FASP) protocol.[8] Endoproteinase Lys-C and trypsin were used for sequential digestion of proteins. The enzyme to protein ratios were 1/50. Lys-C and tryptic peptides from whole lysates were fractionated using pipet tip strong ion exchange separation (SAX) micro columns[10] into two fractions, which eluted at pH 5 and pH 2, respectively. Membrane fractions were analyzed in duplicates without the SAX fractionation (in total, four liquid chromatography tandem spectrometry (LC−MS/MS) runs per sample).

LC−MS/MS Analysis

Analysis of the peptide mixtures was performed using high energy collision dissociation (HCD) fragmentation mode[11] as described previously.[8] Briefly, the peptides were separated on a reverse phase column (20 cm × 75 μm inner diameter) packed with 1.8 μm of C18 particles (Dr. Maisch GmbH, Ammerbuch−Entringen, Germany) using a 4 h acetonitrile gradient in 0.1% formic acid at a flow rate of 250 nL/min. The LC was coupled to a Q Exactive mass spectrometer (Thermo Fisher Scientific, Germany) via a nanoelectrospray source (Proxeon Biosystems, now Thermo Fisher Scientific). The Q Exactive was operated in data-dependent mode with survey scans acquired at a resolution of 50 000 at m/z 400 (transient time 256 ms). Up to the top 10 most abundant isotope patterns with charge ≥ +2 from the survey scan were selected with an isolation window of 1.6 Th and fragmented by HCD with normalized collision energies of 25. The maximum ion injection times for the survey scan and the MS/MS scans were 20 and 60 ms, respectively. The ion target value for both scan modes was set to 10^6. The dymamic exlusion was 25 s and 10 ppm.

Data Analysis

The spectra were searched using the "Andromeda" search engine[12] and analyzed using the MaxQuant software version 1.2.6.20 using the "matching between runs" option.[7] Proteins were identified by searching MS and MS/MS data of peptides against a decoy version of the UniProtKB/Swiss-Prot (May 2013) containing 50 807 sequences. Carbamidomethylation of cysteines was set as a fixed modification. N-terminal acetylation and oxidation of methionines were set as variable modifications. Up to two missed cleavages were allowed. The initial search allowed mass deviation of the precursor ion was up to 6 ppm and for the fragment masses it was 0.5 Da. Mass accuracy of the precursor ions was improved by time-dependent recalibration algorithms of MaxQuant. The "match between runs" option enabled us to match identifications across samples within a time window of 2 min of the aligned retention times. The maximum false peptide discovery rate was specified as 0.01. For relative protein quantitation, the label free quantitation (LFQ) option of the MaxQuant software was used. Significance of outliers was calculated by multiple hypothesis testings[13] with threshold value of 0.05. Protein abundances were calculated on the basis of raw spectral protein intensity that employed the total protein approach (TPA)[14] using the following relationships:

$$Total\ protein\ (i) = \frac{MS\ Signal\ (i)}{Total\ MS\ Signal} \times 100$$

and the protein i concentration

dx.doi.org/10.1021/pr500833v | J. Proteome Res. 2015, 14, 353−365

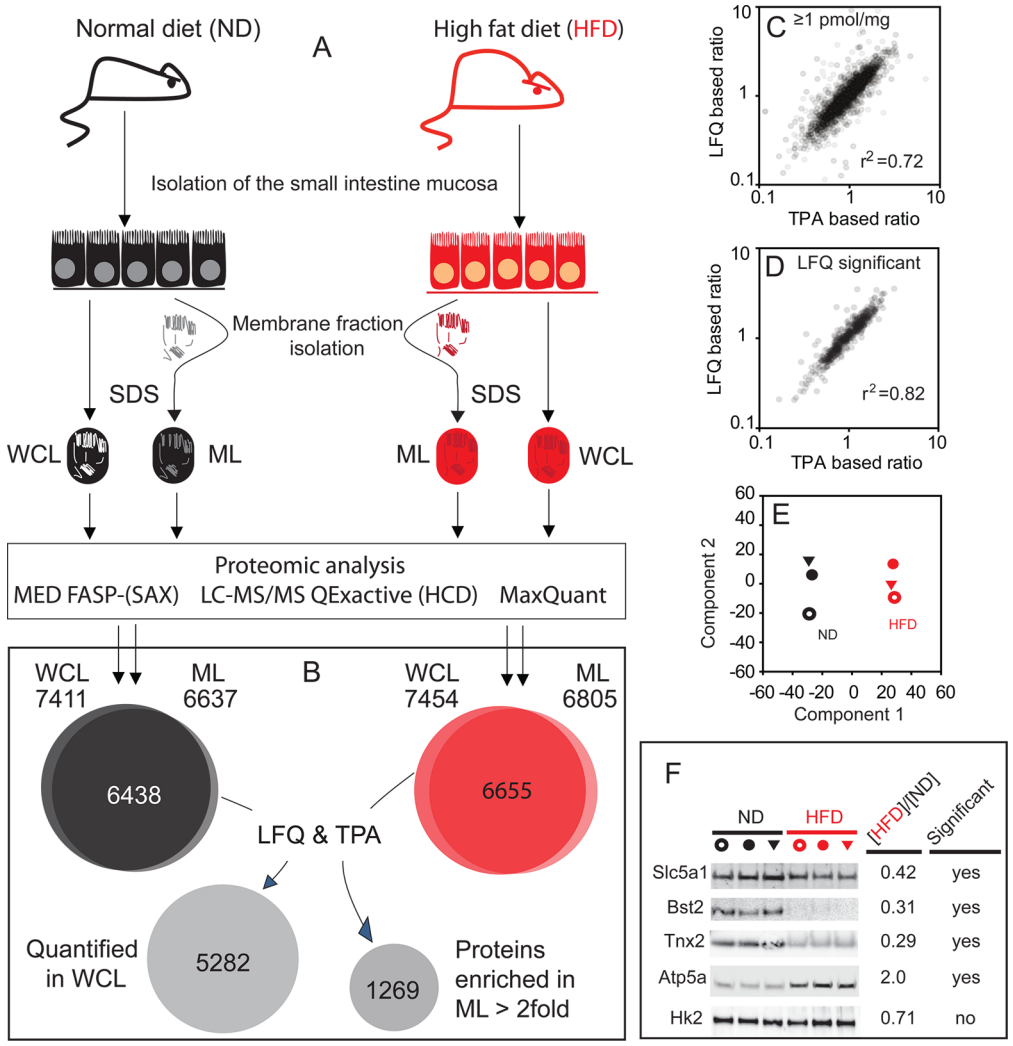

Figure 1. Experimental design and quantitative proteomic analysis. (A) Proteomic workflow. Small intestinal mucosal scraping containing mainly enterocytes were prepared from mice fed with either ND or HFD. The cells were either directly lysed in SDS-containing buffer (WCL) or were used for isolation of cellular membranes (ML). The lysates were processed with the MED-FASP procedure, and the generated peptides were analyzed by LC−MS/MS. The raw data were analyzed using the MaxQuant Software. (B) Identification of proteins. In WCLs of the ND and HFD group, 7411 and 7454 proteins were identified, respectively. In the MLs, 6637 proteins were mapped in the ND group, and 6805 were mapped in the HFD group. In at least two samples of each group, 5282 proteins were quantified using the LFQ module of the MaxQuant software, and their absolute abundances (protein content and molar concentration in the cells) were calculated by means of the TPA. (C,D) Correlation of the protein abundance ratios calculated with the LFQ and TPA methods. The 2200 most abundant proteins (≥1 pmol/mg of total protein) were compared. (E) Principal component analysis of the proteomes quantified after ND and HFD; 564 significantly changed proteins were analyzed. ND, black symbols; HFD, red symbols. The open and closed circles and the triangles used in the different panels (and other figures) refer to individual samples. (F) Western blot analysis. WCLs, each from ND and HFD, were separated by SDS-polyacrylamide gel electrophoresis (PAGE) and blotted onto nitrocellulose membrane, and the bots were probed with antibodies. Each lane corresponds to an individual lysate analyzed by LC−MS/MS.

$$C\ (i) = \frac{MS\ signal}{Total\ MS\ Signal \times MW}$$

in [mol/(g of total protein)]. The calculations were performed in Microsoft Excel.

RESULTS

Quantitative Mapping of the Proteome of Small Intestinal Mucosa

Small intestinal mucosa was isolated from male mice that were fed for two months postweaning with a ND containing 29.0% polysaccharides, 5.4% disaccharides, 19.6% protein, 4.1% fiber, and 3.3% fat or with a HFD containing 15.8% polysaccharides, 9.5% disaccharides, 24.1% protein, 6% fiber, and 34.6% fat. After feeding for two months with HFD the body weight of the mice is about 30% higher compared to that of the mice on ND, and the mice show an increased serum glucose peak during the oral glucose tolerance test and an increased insulin concentration in the blood after fasting, which indicates a prediabetic state.[15] To see whether the HFD may alter transporter activities in the enterocytes, we compared SGLT1-mediated glucose uptake in everted small intestinal rings of male mice that were starved overnight. After HFD, the uptake of 10 μM [^{14}C]α-methyl D-glucopyranoside (AMG) inhibited by 1 mM phlorizin, which is mediated by SGLT1(gene *Slc5a1*),[16] was inhibited by 19.8 ± 4.6% (mean ± standard error of the mean (SEM), n = 14 each group, $P < 0.01$ for difference). To analyze the HFD-dependent changes of the protein composition in the mucosa, male mice were starved overnight and sacrificed in the morning.

dx.doi.org/10.1021/pr500833v | J. Proteome Res. 2015, 14, 353−365

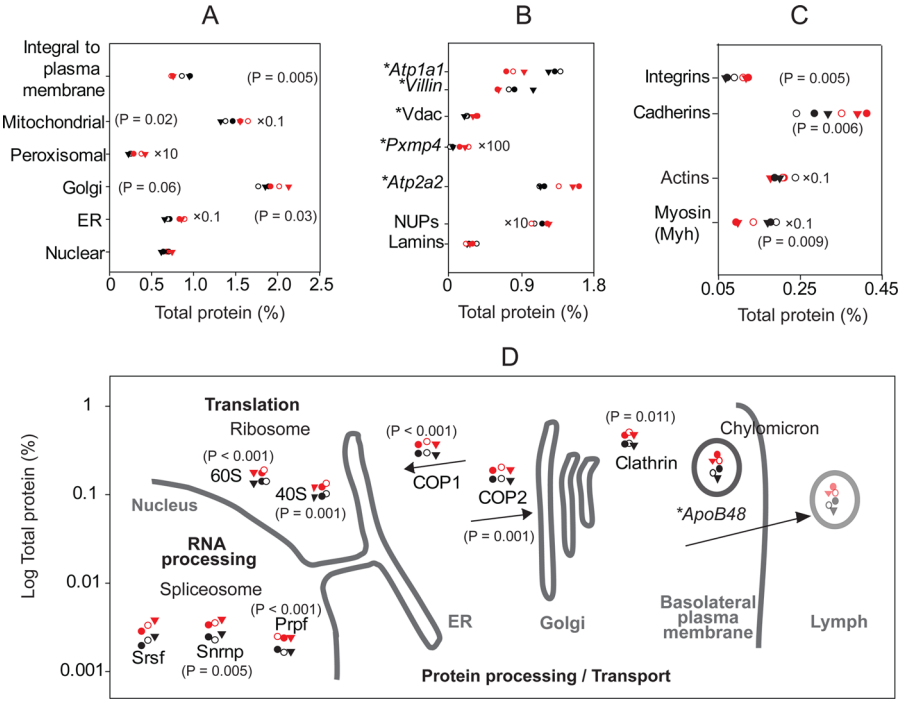

Figure 2. HFD-related changes in the architecture of the enterocytes. ND, black symbols; HFD, red symbols. (A) Sum of proteins from different intracellular compartments after ND or HFD measured in WCLs and presented as percentage of the total protein. (B) Abundances of individual membrane-associated proteins or groups of membrane-associated proteins after ND or HFD presented as percentage of total protein in WCLs. (C) Comparison of expression of integrins, cadherins, actins, and mysosin after ND or HFD; × 0.1, × 10, and ×100 indicate that the values were multiplied by 0.1, 10, or 100, respectively. (D) Abundances of proteins involved in RNA processing, translation, and protein and lipid transport after ND or HFD (note logarithmic scale of the "Total protein" values). The open and closed circles and the triangles used in the different panels refer to individual samples. Asterisks indicate significant protein changes of individual proteins in the LFQ analysis (Table 2, Supporting Information). *P*-values of changes between specific groups of proteins are given in parentheses. Nonsignificant changes are not indicated.

The jejunum was dissected and everted, and the mucosa was removed by scraping with a glass plate. The mucosal scrapings containing the enterocytes and part of the submucosal layer were homogenized (whole cell fraction), or membranes were isolated by differential centrifugation. The samples were lysed in SDS-containing buffer containing protease inhibitors. The WCLs and the MLs were processed using the FASP procedure[6] that employed consecutive protein digestion with endoproteinase LysC and trypsin[8] (MED-FASP) (Figure 1A). To increase the proteome coverage of the WCL analysis, the LysC and tryptic peptides were additionally separated into two fractions using SAX pipet tip columns prior to LC–MS/MS.[10] The spectra were processed using MaxQuant software.[7] In the WCL samples from mice on ND or HFD, 7411 and 7454 proteins were identified, whereas 6637 or 6805 proteins were identified in the ML samples of mice fed with ND and HFD, respectively (Figure 1A and Table 1, Supporting Information). Only 3% of the proteins found in the MLs were not matched in the WCLs; most of these are lower abundant membrane proteins. To compare the abundances of proteins between the ND and HFD groups, we used the LFQ modus of the MaxQuant software. For estimation of the protein concentrations, the TPA method was employed. Both methods revealed a good correlation for the ratios of protein levels between ND and HFD animals (Figure 1C,D). For selected proteins, the titer ratios were validated using Western blots (Figure 1F).

The final data set of quantified proteins in WCL samples comprises 5282 proteins that were identified in at least two of three samples in both ND and HFD animals (Table 2, Supporting Information). On the basis of *t* test analysis of the LFQ data, more than 10% of the proteins were significantly changed, with $p < 0.05$ between ND and HFD animals (Table 2, Supporting Information). Principal component analysis of the data showed a stringent separation of both groups of samples (Figure 1E) and revealed several protein classes with significant changes after HFD (Table 3, Supporting Information). Comparison of the protein titers in the ML and WCL samples allowed discrimination between proteins that were enriched in the membrane fraction. More than 1200 proteins were more than two-fold enriched or identified only in the membrane fractions (Figure 1B and Table 4 of the Supporting Information). The analysis allowed the identification and quantification of 88 different plasma membrane transporters in the enterocytes (Table 5, Supporting Information). The fatty acid transporter FATP2 (gene *Slc27a2*),[17] the choline transporter CLT1 (gene *Slc44a1*),[18] the orphan transporter homologue ORCTL2 (gene *Slc22a18*),[1] and the gene product of *Slc22a23*[1] have not been detected in small intestine before. The performed quantification of transporter expression provides information about the potential functional relevance of the individual transporters, for example, the highest expression was observed for the α-subunit of the Na,K-ATPase, which is located in the BLM of the enterocytes (gene *Atp1a1*, 117 pmol/mg WCL). The next two most abundantly expressed transporters in the BLM of the enterocytes are the amino acid transporter LAT2 (gene *Slc7a8*, 6.2 pmol/mg WCL) and the H^+-monocarboxylate cotransporter MCT1 (gene *Slc16a1*, 5.3 pmol/mg WCL). The three most abundantly expressed transporters of the BBM are the Na^+-D-glucose cotransporter SGLT1 (gene *Slc5a1*, 30.4 pmol/mg WCL), the fatty acid

dx.doi.org/10.1021/pr500833v | J. Proteome Res. 2015, 14, 353–365

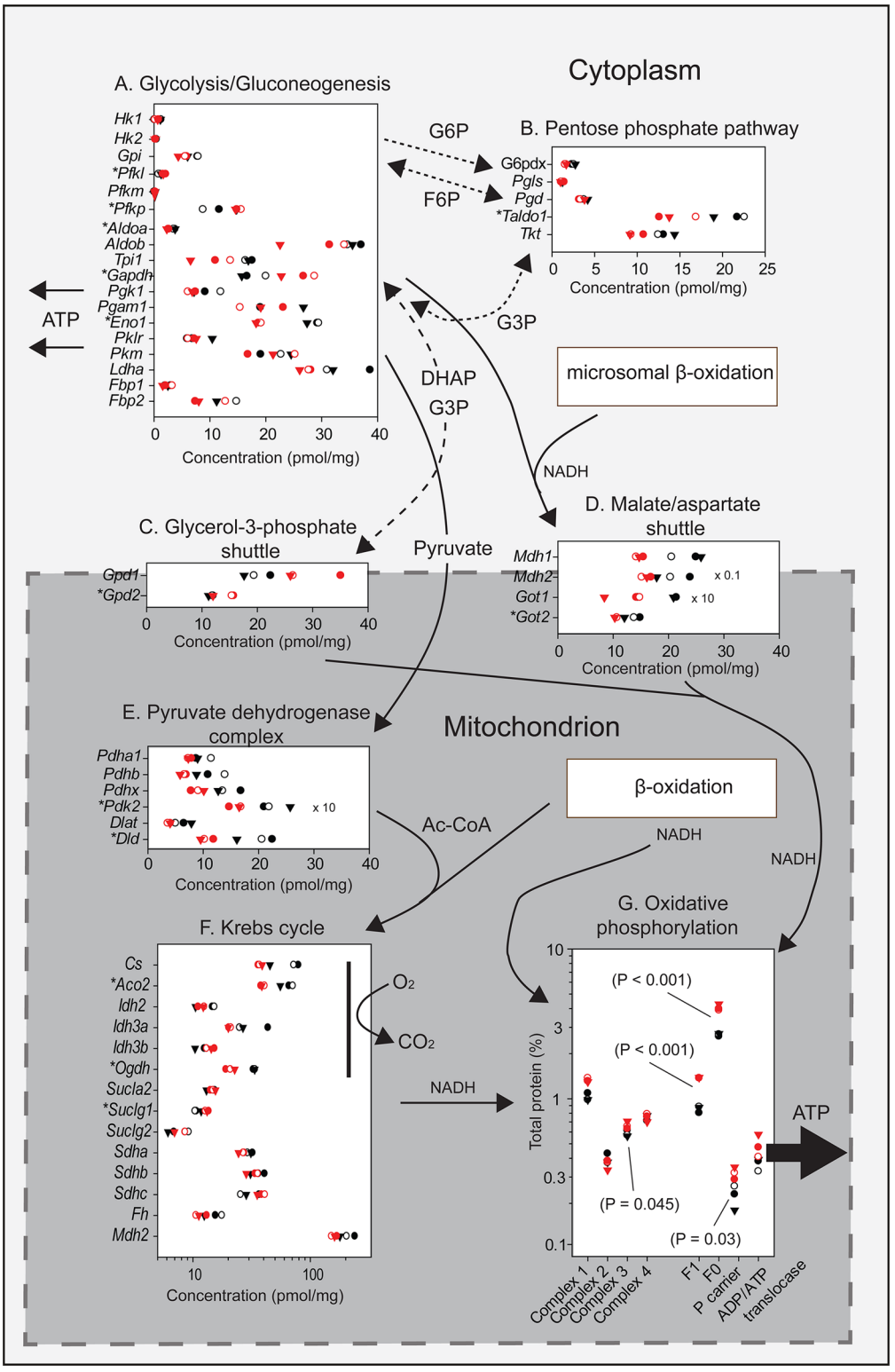

Figure 3. Effect of HFD on abundances of the proteins involved in main catabolic pathways. ND, black symbols; HFD, red symbols. (A) Comparison of enzymes involved in glycolysis and gluconeogenesis after ND or HFD. (B) Comparison of enzymes involved in pentose phosphate pathway after ND or HFD. (C) Comparison of proteins of the glycerol phosphate shuttle after ND or HFD. (D) Comparison of proteins involved in malate/aspartate shuttle after ND and HFD. (E) Abundance of components of the pyruvate dehydrogenase complex after ND and HFD. (F) Abundance of enzymes of the Krebs cycle after ND and HFD. (G) Comparison of proteins involved in oxidative phosphorylation after ND and HFD. The open and closed circles and the triangles used in the different panels refer to individual samples. Asterisks indicate significant protein changes of individual proteins in the LFQ analysis (Table 2, Supporting Information). *P*-values of changes between specific groups of proteins are given in parentheses. Nonsignificant changes are not indicated.

dx.doi.org/10.1021/pr500833v | *J. Proteome Res.* 2015, 14, 353−365

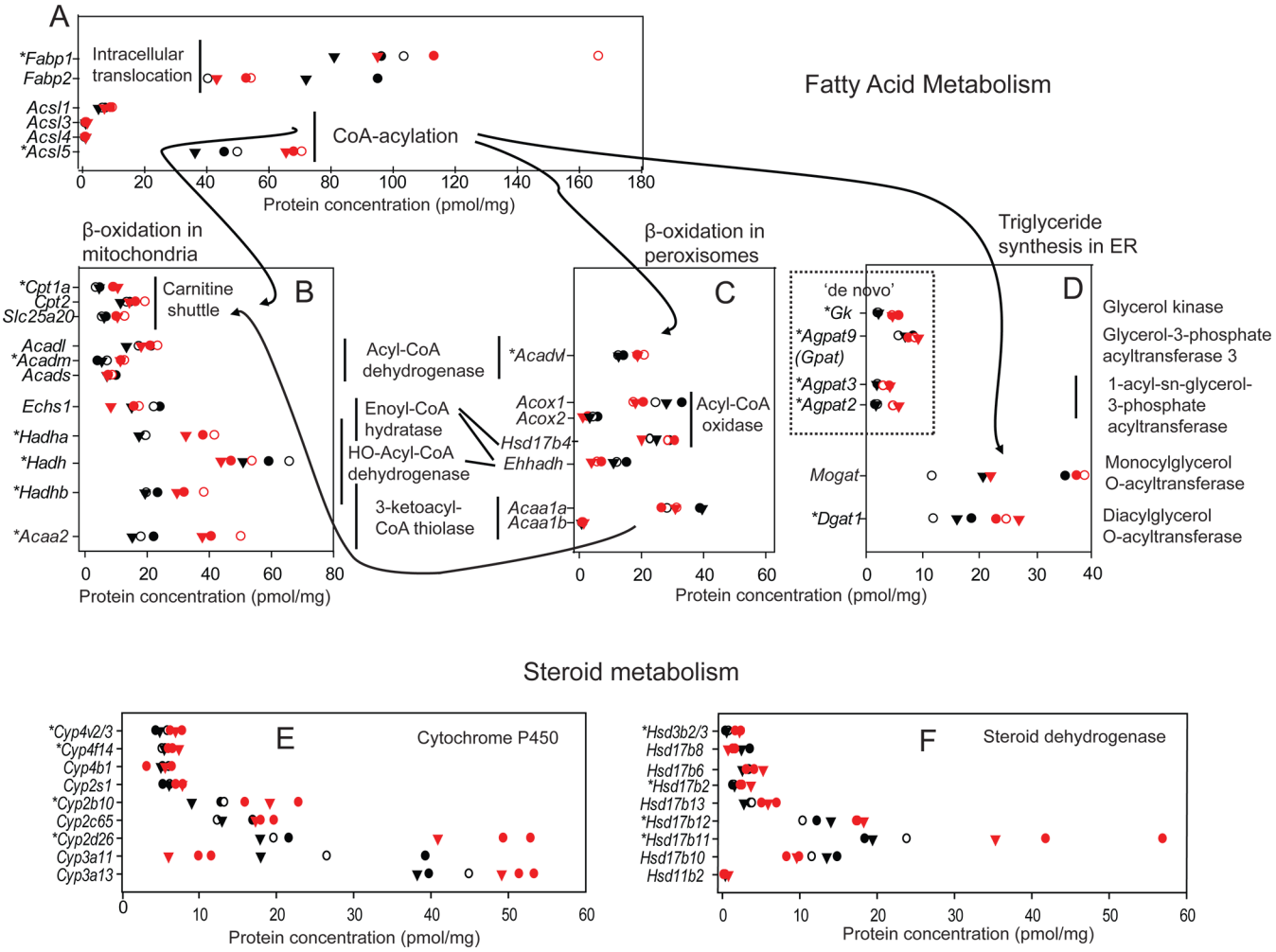

Figure 4. Effect of HFD on expression of proteins involved in lipid metabolism. ND, black symbols; HFD, red symbols. (A) Cytoplasmic translocation via fatty acid binding proteins and CoA acylation via ligases. (B) Mitochondrial beta-oxidation. (C) Peroxisomal beta-oxidation. (D) Triglyceride synthesis from monoacylglycerate and via the "de novo" pathway. (E) Steroid oxidation by cytochrome P450 oxidases. (F) Reduction of steroids by steroid hydrogenases. The open and closed circles and the triangles used in the different panels refer to individual samples. Asterisks indicate significant protein changes of individual proteins in the LFQ analysis (Table 2, Supporting Information). Nonsignificant changes are not indicated.

transporter FATP4 (gene *Slc27a4*, 19.7 pmol/mg WCL), and the H^+-peptide cotransporter PEPT1 (gene *Slc15a1*, 4.86 pmol/mg WCL). Since the oral absorption of hydrophilic drugs is mediated by polyspecific drug transporters in the BBM and BLM, it is important to know the expression level of these transporters in the enterocytes. Concerning drug transporters localized in the BBM, we observed that the ATP-dependent export pump for neutral and positively charged compounds MDR1a (gene *Abcb1a*, 4.31 pmol/mg WCL) was six times higher than the ATP-dependent export pump MRP2 (gene *Abcc2*, 0.69 pmol/mg WCL) and seven times higher than the organic cation transporter OCT1 (gene *Slc22a1*, 0.58 pmol/mg WCL) that mediates the uptake of organic cations. Interestingly, we did not detect the H^+-organic cation antiporter OCTN1 (gene *Slc22a5*), which was considered to be involved in the efflux of cationic drugs across the BBM.[19]

HFD Induces Changes of Ultrastructure, Compartmentation, Cell–Cell Contacts, and Adhesion of Enterocytes

Because changes of 11% of the proteome may be reflected in varied composition of different subcellular compartments, we took a closer look at cell organelle specific proteins. After HFD, the content of total integral plasma membrane proteins was decreased, whereas the overall abundances of mitochondrial proteins, proteins of the Golgi complex, proteins of the endoplasmic reticulum (ER), and proteins of the peroxisomes were increased (Figure 2A and Table 6 of the Supporting Information). In contrast, the content of proteins associated with the nuclear membrane remained almost unchanged (Figure 2A). Examples of HFD-dependent overall changes of proteins in subcellular compartments are shown in Figure 2, panel B and Table 6 of the Supporting Information. The abundantly expressed α-subunit of the Na,K-ATPase (gene *Atp1a1*) in the basolateral plasma membrane of the enterocytes and villin in the BBM were down-regulated. The voltage-dependent anion channel (VDAC) in the outer mitochondrial membrane (genes *Vdac1*–*3*), the peroxisomal membrane protein 4 (gene *Pxmp4*), and the Ca-ATPase in the ER (gene *Atp2a2*) were up-regulated, whereas the concentrations of nuclear pore complex proteins (NUPs, *NUP* genes) and lamins (*Lma and Lmb* genes) were not changed significantly.

We wondered whether HFD-induced changes in protein expression influence cell adhesion, cell–cell contacts, structure

dx.doi.org/10.1021/pr500833v | J. Proteome Res. 2015, 14, 353–365

of microvilli, or motility of microvilli. Figure 2, panel C indicates that HFD increased the expression of integrins that mediate cell adhesion and the expression of cadherins, which are critical components of cell−cell contacts. The expression of actin filaments, which establish the structural core of the microvilli, was not changed; however, the expression of motor protein myosin, which is located in the terminal web of the enterocytes and mediates movements of the microvilli, was decreased. Our data suggest that cellular adhesion and cell−cell interactions are increased after HFD, whereas the movements of the microvilli are decreased.

HFD Affects Protein Synthesis and Cellular Transport of Proteins

Principal component analysis (PCA) revealed that the abundances of proteins that are involved in transcription and processing of RNA and in the synthesis, modification, and processing of proteins were increased (Table 3, Supporting Information). In Figure 2, panel D, abundances of representative proteins that are parts of large protein complexes and are involved in processing and transcription of RNA and in protein synthesis are shown. Following the protein expression path, up-regulation of spliceosomal and ribosomal assemblies (Figure 2D) suggests elevated RNA synthesis, processing, and translation in the HFD animals. Increased abundances of the coat protein complexes COP1 and COP2 (Figure 2D) correlate with augmented shuttling of proteins and lipids between the ER and Golgi. Clathrins are major components of the clathrin-coated secretory vesicles. Their up-regulation suggests elevated protein secretion. All of these observations together indicate an orchestrated increase in protein synthesis in the enterocytes exposed to HFD. Finally, we observed a significant increase in the titer of apolipoprotein 48 (ApoB48), a key component of chylomicrons that exports triglycerides from the enterocytes to the lymph.

Synthesis of dolichol−P-P-$GlcNAc_2Man_9Glc_3$ is the initial step in N-glycosylation of proteins in the ER. After HFD, the abundances of most enzymes involved in this synthesis were increased (Figure 1, Supporting Information, left panel). Accordingly, also the proteins of the oligosaccharyltransferase (OST) complex were up-regulated (Figure 1, Supporting Information), which suggests elevated attachment of the N-glycan precursor to nascent proteins, but we did not observe any impact of HFD on enzymes promoting maturation of N-glycosylation in the Golgi. We do not know whether the capacity of these downstream events in N-glycosylation is sufficiently high to carry out the glycan-conversions in the Golgi or whether some proteins end up with premature glycosylation.

Oxidative Energy Metabolism Is Amplified in HFD on the Main Catabolic Pathways

Higher fat uptake during HFD compared to ND resulted in widespread changes in catabolic metabolism in the enterocytes. The concentrations of many enzymes involved in glycolysis, pentose phosphate pathway, and the Krebs cycle were reduced (Figure 3A,B,F), whereas several glycolytic enzymes such as aldolase A (*Aldo A*) and enolase (*Eno1*) were significantly down-regulated; glyceraldehyde-3-phosphate dehydrogenase (*Gapdh*) was significantly up-regulated. This may be explained by the fact that *Gapdh* is not only part of the glycolytic pathway, but also involved in the metabolism of glycerol, which is liberated from triglycerides.

Because of the down-regulation of glycolytic enzymes, the synthesis of pyruvate and reduced nicotinamide adenine dinucleotide (NADH) by glycolysis may be decreased. This is consistent with the HFD-induced down-regulation of components of the malate/aspartate shuttle, which mediates translocation of cytoplasmic NADH into mitochondria and with the down-regulation of the proteins that assemble the mitochondrial pyruvate dehydrogenase complex (Figure 3D,E). Expression of enzymes involved in energy production by carbohydrate catabolism was decreased after HFD, but the expression of various enzymes that are involved in catabolism of triglycerides, steroids, and fatty acids was increased (see below and Figure 4). Although this suggests an increased supply of acyl-CoA to the Krebs cycle after HFD, the expression of Krebs cycle enzymes was not increased consistently (Figure 3). On the other hand, the expression of transporters for Krebs cycle intermediates in the inner mitochondrial membrane was increased. The expression of the citrate−malate exchanger CTP (*Slc25a1*) and the 2-oxoglutarate-malate exchanger OGC (*Slc25a11*) were increased by 55% and 60%, respectively. Overall, the energy supply to the mitochondria may be increased after HFD. Ten components of the respiratory chain were up-regulated 1.6−3.9-fold after HFD (Figure 3G and Table 2 of the Supporting Information), which suggests an increased oxidative phosphorylation. Statistically significant increased expression was observed for seven NADH dehydrogenase components of mitochondrial complex 1 (*Ndufa10, Ndufb10, Ndub4, Ndub7, Ndufs2, Ndufs3, NdufsS*), a subunit of cytochrome C oxidase in complex 3 (*Cox4i1*), subunits of the ATP synthase (F1-complex α-subunit 1 (*Atp5a1*), and F_0 complex subunit E (*ATP5i*) (Table 2, Supporting Information).

HFD Up-Regulates Lipid Absorption and Metabolism

After HFD, the expression of many proteins that participate in small intestinal absorption and metabolism of lipids was changed (Figure 4). In the small intestinal lumen, dietary triglycerides (TGs) are hydrolyzed by pancreatic lipases into two fatty acids (FAs) and one sn-2-monoacyl glycerol. These products enter the enterocytes across the BBM via passive diffusion and transporters, partially bind to cytosolic proteins for intracellular movement (see Fabp1, Fabp2 in Figure 4A), and are mainly resynthesized to TGs in the ER (Figure 4D). The resynthesized TGs are packed into chylomicrons and released to the interstitium by exocytosis (Figure 2D). A fraction of the cytosolic FAs is catabolized by β-oxidation in mitochondria and peroxisomes (Figure 4B,C). Processing of FAs is always initiated by activation of FAs via CoA by FA-CoA ligases. The expression of FACL5 (*Acsl5*), the most abundant acyl-CoA-synthetase in the enterocytes, was increased 1.8-fold after HFD (Figure 4A). After HFD, also the expressions of several proteins that are involved in mitochondrial β-oxidation were significantly increased (Figure 4B). The expression of carnitine palmitoyltransferase 1A (*Cpt1a*), which is involved in carnitine shuttle of FAs into the mitochondria, was increased by 144%; that of both subunits of hydroxyacyl-CoA dehydrogenase (*Hadha, Hadhb*) was increased by about 100%; and that of acyl-CoA dehydrogenases for short and long FAs (*Acadm, Acadl*) was increased by about 100%. In contrast to mitochondria, proteins that carry out β-oxidation of very large FAs in the peroxisomes were less abundant after HFD (Figure 4C). Apparently, in HFD, the very large chain FAs are preferentially re-esterified into TGs instead of being metabolized for mitochondrial oxidation.

dx.doi.org/10.1021/pr500833v | J. Proteome Res. 2015, 14, 353−365

Table 1. Plasma Membrane Transporters with Significantly Different Expression after HFD and ND

gene	protein	location	transport mechanism	substrates	concentration ratio HFD/ND
Abcc3	MRP3	BLM[a]	ATP-dep. export	drugs, drug metabolites, xenobiotics, anions	0.64
Abcg2	BCRP	BBM	ATP-dep. export	drugs (many chemotherapeutics), xenobiotics	0.33
Abcg5	Sterolin 1	BBM	ATP-dep. export	sterols, drugs, xenobiotics	0.60
Atp1a1	Na,K-ATPase	BLM	ATP-dep. exchange	sodium, potassium	0.64
Slc2a2	GLUT2	BLM	facilitated diffusion	D-glucose	0.31
Slc2a5	GLUT5	BBM	facilitated diffusion	fructose	1.85
Slc4a4	NBCe1	BLM	Na-cotransport	sodium, bicarbonate	0.46
Slc5a1	SGLT1	BBM	Na-cotransport	D-glucose, D-galactose	0.42
Slc5a8	SMCT1	BBM	Na-cotransport	short chain fatty acids	0.15
Slc13a2	NaDC1	BBM	Na-cotransport	succinate, citrate, α-ketoglutarate	0.52
Slc15a1	PEPT1	BBM	H-cotransport	dipeptides, tripeptides, drugs	0.34
Slc16a10	TAT1	BLM	facilitated diffusion	aromatic amino acids	0.56
Slc27a2	FATP2	n.d.	n.d.	long chain fatty acids	2.34
Slc31a1	CTR11	BBM	n.d.	copper, cisplatin	0.61
Slc34a2	NaPI-IIb	BBM	Na-cotransport	inorganic phosphate (divalent)	0.25
Slc44a4	CTL4	n.d.	Na-cotransport	choline	0.30

[a]n.d., Not determined.

In the ER, TGs are synthesized via two pathways, the sn-2-monoacyl glycerol pathway and the de novo glycerol phosphate pathway (Figure 4D). The enzymes involved in the first one are several times more abundant than those of the second one. Both pathways were up-regulated after HFD.

Besides FAs and TGs, steroids represent the second major group of dietary lipids. Our proteomic analyses led to the identification and quantitation of a number of cytochrome P450-oxidases (Figure 4E) and dehydrogenases (Figure 4F), which are involved in steroid metabolism. The majority of these enzymes have higher titers in the HFD than in the ND, which suggests elevated breakdown or conversion of steroids. Many of these enzymes are involved in the metabolism of drugs.

Effect of HFD on the Expression of Plasma Membrane Transporters

In small intestine nutrients, xenobiotics and drugs are absorbed via transporter-mediated uptake across the BBM and transporter-mediated efflux across the BLM of the enterocytes. Since metabolism of the enterocytes is influenced by cytosolic concentrations of nutrients, a changed expression level of nutrient transporters in the plasma membrane may be correlated with changed expression levels of metabolic enzymes. In addition, changed expression levels of plasma membrane transporters may lead to changes in small intestinal absorption. Table 1 shows that the expression of 16 plasma membrane transporters was changed by HFD, 14 of them were down-regulated, whereas two were up-regulated. Importantly, the most abundant plasma membrane transporter in the enterocytes, the Na,K-ATPase in the BLM (Table 1), which provides the driving force for the Na-cotransporters, was down-regulated after HFD. The Na^+-D-glucose cotransporter SGLT1, which is mainly responsible for the uptake of D-glucose across the BBM and the passive glucose transporter GLUT2, which mediates glucose efflux out of the enterocytes across the BLM, were also down-regulated. HFD-dependent down-regulation was also observed for Na^+-cotransporters for short chain FAs (SMCT1), dicarboxylates (NaDC1), and phosphate (NaPi-IIB) in the BBM; the H-peptide cotransporter PEPT1 in the BBM; and the copper transporter CTR11 in the BBM. Also the amino acid transporter TAT1, the Na-bicarbonate cotransporter NBCe1, and the ATP-dependent exporter for organic anions MRP3 in the BLM were down-regulated. The data suggest that small intestinal absorption of D-glucose, amino acids, short chain FAs, choline, and phosphate are decreased after HFD. The expressions of transporter FATP2, which transports long chain FAs and of the fructose transporter GLUT5 were increased after HFD. The decreased expression of the Na,K-ATPase of SGLT1 and of GLUT2 suggests a reduced small intestinal glucose absorption and a decreased intracellular concentration of glucose, which is consistent with the observed down-regulation of the glycolytic enzymes. The up-regulation of FATP2 is consistent with observed increased catabolic metabolism of FAs.

Since small intestinal absorption of many oral drugs and ingested xenobiotics is partially mediated via polyspecific drug transporters in the plasma membrane of enterocytes, the HFD effect on the expression deserves special note. After HFD, two ATP-dependent export transporters for drugs and xenobiotics in the BBM (BCRP and the gene product of *Abcg5*), one ATP-dependent export transporter for drugs and xenobiotics in the BLM (MRP3), the H-peptide cotransporter PEPT1, which translocates lactam antibiotics in the BBM, and the copper transporter CTR11 in the BBM, which accepts cisplatin as substrate are down-regulated (Table 1).

Effect of HFD on Proteins Involved in Metabolism of Drugs and Xenobiotic

In addition to the liver, the small intestine plays an important role in the metabolism of drugs and xenobiotics. Orally ingested compounds often undergo a first pass metabolism within small intestinal enterocytes. The compounds may be oxidized and metabolized or modified by glucuronidation, sulfation, phosphorylation, or transesterification. Unmodified or modified compounds may be extruded by the ATP-dependent export pumps. The export pumps MDR1, BRCP, and MRP2 mediate export across the luminal membrane, whereas the export pump MRP3 mediates translocation across the BLM. In combination with the intracellular metabolizing and conjugating enzymes, the luminal export pumps serve as metabolic barriers for drugs and xenobiotics.[20] Some drugs or drug metabolites in the blood that are excreted into bile are reabsorbed in the small intestine. In addition, the small intestine may secrete drugs or drug metabolites into the intestinal lumen.

In our proteome analysis, many enzymes involved in small intestinal drug metabolism were identified and quantified. The

dx.doi.org/10.1021/pr500833v | J. Proteome Res. 2015, 14, 353−365

Table 2. Drug Metabolizing Enzymes with Significantly Different Expression after HFD and ND

gene	protein, enzymatic activity/subcellular location	protein concentration after ND mean ± SD (pmol/mg)	concentration ratio HFD/ND
Aadac	arylacetamide deacetylase/mitochondria	7.57 ± 1.51	3.29
Adh1	alcoholdehydrogenase 1/cytosol	6.36 ± 1.21	3.35
Aldh3a2	aldehydedehydrogenase 3a2/ER	6.82 ± 0.74	3.21
Cbr1	carbonylreductase 1/mitochondrial	8.69 ± 1.15	3.51
Ces2e	carboxyesterase 2E/ER	69.4 + 13.8	0.57
Ces2g	carboxyesterase 2G/ER	3.26 ± 0.41	0.50
Ces3	carboxyesterase 3/ER	8.77 ± 2.30	0.34
Cyp2b10	CYP2B10 monooxygenase/ER	11.7 ± 2.33	1.82
Cyp2d26	CYP2D26 monooxygenase/ER	19.8 ± 1.87	2.14
Cyp4f14	CYP4F14 monooxygenase/ER	5.48 ± 0.21	1.27
Cyp4v3	CYP4 V3 monooxygenase/ER	5.11 ± 0.77	1.47
Dhrs1	dehydrogenase−reductase 1/peroxisome	19.2 ± 1.87	2.12
Dhrs3	dehydrogenase−reductase 3/not determined	0.30 ± 0.02	4.54
Dhrs4	dehydrogenase−reductase 4/peroxisome	9.69 ± 3.60	3.08
Dpyd	dihydropyrimidine dehydrogenase/cytosol	1.25 ± 0.20	0.68
Fmo4	flavin-containing monooxygenase 4/ER	3.28 ± 0.22	2.09
Fmo5	flavin-containing monooxygenase 5/ER	13.5 ± 2.29	1.90
GM3776	GM3776g gluthation-*S*-transferase alpha/cytosol	25.3 ± 4.41	0.42
Maob	monoamine oxidase B/mitochondria	10.3 ± 2.50	2.09
Marc2	amidoxime-reducing component 2/mitochondria	57.3 ± 9.29	1.99
Papss1	PAPSS1 sulfotransferase/cytosol	1.09 ± 0.22	0.37
Por	CPR, cytochrome P450 monooxygenase/ER	8.64 ± 1.14	2.49
Ptgs1	prostaglandin−endoperoxide synthase 1	0.65 ± 0.16	2.63
Ugt2b34	UDP glucuronosyltransferase 2 polyp. B34/ER	12.2 ± 1.61	1.90

Table 3. Expression of Proteins Involved in Enterocytes Related Immune Reactions and Stimulation of Immune Cells after HFD

gene	protein/function	concentration ratio HFD/ND
Bst2	bone marrow stromal cell antigen 2/facilitates growth of pre-B-lymphocytes	0.31
Cd74	CD74 molecule, invariant chain of MHCII/antigen presentation	0.22
Ctsa	catepsin A/associated with beta-galactosidase, supports maturation of MHCII	0.45
Dpp4	dipeptidylpeptidase 4 is identical to T-lymphocytes activating antigen CD26	0.46
Ece1	endothelin converting enzyme 1/regulation of immune cells	0.50
Exosc6	exosome component 6/IgG class switch recombination, IgG variable region hypermutation	0.41
Exosc7	exosome component 7/IgG class switch recombination, IgG variable region hypermutation	0.41
H2-Aa	H2-class II histocompatibility antigen, A-B alpha/antigen presentation in immune cells	0.21
H2-Ab1	H2-class II histocompatibility antigen, A beta/antigen presentation in immune cells	0.20
Igj	immunoglobulin j-chain/component of IgA and IgM, humoral immune response	0.31
Igk-V19−17	Ig kappa chain V19−17/light chain of immunoglobulins, humoral immune response	0.14
P01837	Ig kappa chain C-region of/light chain of immunoglobulins, humoral immune response	0.54
Lcp1	lymphocyte cytosolic prot. 1/actin-binding protein, role in T-cell response to costimulation	0.48
Lgals3	lectin−galactose binding sol. 3/binds to IgE, activates neutrophilic granulocytes	0.72
Lyn	tyrosine kinase/regulation of immune response, inflammation	0.59
Mst1r	receptor for macrophage-stimulating protein 1/stimulates macrophages	0.56
Pabpc4	poly A binding prot. cytoplasmic 4/increases mRNA stability in activated T-lymphocytes	0.47

data indicated dramatic species differences between mouse and man, for example, we detected none of the cytochrome P450 enzyme subtypes described in human intestine in mice and vice versa.[21,22] We identified three alcohol dehydrogenases (*Adh1*, *Adh5*, *Adh6a*), nine aldehyde dehydrogenases (*Aldh1a1*, *Aldh1a3*, *Aldh1a7*, *Aldh1b1*, *Aldh2*, *Aldh3a2*, *Aldh3b1*, *Aldh7a1*, *Aldh9a1*), 26 cytochrome P450-type monooxygenases (*Cyp2*, *3*, *4*, *27*, *51* subtypes and *Por*), and three flavin-containing FMO monooxygenases (*Fmo2*, *Fmo4*, *Fmo5*) (Table 7, Supporting Information). The alcohol dehydrogenases ADH-I and ADH6A are abundantly expressed. After HFD, the expression of ADH1 was increased 3.4-fold (Table 2). The most abundantly expressed aldehyde dehydrogenase was ALDH1B1, followed by ALDH2 and ALDH1A1 (Table 7, Supporting Information). After HFD, the expression of ALDH3A2, which was expressed at a 14-fold lower level compared to ALD1B1, was increased 3.2-fold (Table 2). CYP3A13, CYP3A11, CYP2D26, FMO5, CYP2C65, and CYP2C29 were the most abundantly expressed monooxygenases (Table 7, Supporting Information). Expression of the well-expressed monooxygenases CYP2B10, CYP2D26, CYP4F14, CYP4 V3, FMO4, and FMO5 was increased 1.9 ± 0.4-fold (mean ± SD) (Table 2). In mouse small intestine, we also identified the two mitochondrial carbonyl reductases CBR1 and CBR4 (Table 7, Supporting Information). After HFD, the concentration of strongly expressed CBR1 was increased 3.5-

dx.doi.org/10.1021/pr500833v | *J. Proteome Res.* 2015, 14, 353−365

fold (Table 2). Nine UDP-glucuronosyltransferases located in the ER (*Ugt1* and *Ugt2* subtypes) were identified (Table 7, Supporting Information). UGT1A7C, UGT2B34, and UGT1A1 were expressed most abundantly. After HFD, the expression of UGT2B34 was increased 1.9-fold (Table 2). We also observed the expression of nine carboxyesterases (genes *Ces1*, *2*, *3* subtypes), which are also located in the ER as well as 13 cytosolic glutathione-*S*-transferases (*Gsta*, *k*, *m*, *o*, *p*, *t*, *z* subtypes and *Gm3776*) (Table 7, Supporting Information). The carboxyesterases CES2E, CES2C, CES1F, CES2A, and CES3 and the glutathione-*S*-transferases Gm3776, GSTP1, GSTO1, and GSTK1 were expressed abundantly (Table 7, Supporting Information). After HFD, expression of CES3 was decreased three-fold, and expression of GM3776 was decreased 2.5-fold (Table 2). After HFD, the oxidation of drugs in the phase 1 metabolism is increased. Although glucuronidation of drugs may be also increased, sulfation and modification with glutathione may be decreased.

Alterations in Immune Defense and Tolerance

Important functions of the small intestine are immune defense against pathogenic bacteria and the establishment of tolerance to food and microbial antigens.[23−25] Small intestinal defense includes innate immunity of the complement system, secretion of antibacterial defensins by Paneth cells, secretion of antibodies at the mucosal surface, and presentation of antigens at the BLM for activation of regulatory T-lymphocytes mediating immune tolerance.[23] For induction of immune tolerance, endocytosed proteins become associated with major histocompatibility complex II (MHCII) proteins and are packed together with MHCII proteins into tolerosomes, which leave the enterocytes at the BLM via exocytosis and activate lymphocytes.[23,24]

After HFD, we observed no significant changes of proteins involved in the complement system and of defensins (Table 8, Supporting Information); however, after HFD, the expression of 17 proteins that are directly or indirectly involved in immune defense or immune tolerance was significantly decreased (Table 3). A 78−80% decrease was observed for three components of the MHCII (see *Cd74*, *H2-Aa*, and *H2-Ab1* in Table 3). The expression levels of the four additional proteins of the MHCII detected in the WCLs were decreased by 40−85%; however, the changes of the individual protein expressions did not reach significance (Table 8, Supporting Information). Cathepsin A, which supports maturation of the MHCII was significantly decreased by 55% after HFD. A significant 46−84% decrease in expression after HFD was also observed for three components of immunoglobulins (see *Igj*, *Igk-V19−17*, and P01837 in Table 3). After HFD, also the expression of three proteins that are involved in the maturation or function of T-cells were significantly decreased by 52−54% (see *Dpp4*, *Lcp1*, *Pabpc4* in Table 3). In addition, the expression levels of proteins that stimulate the proliferation of B-lymphocytes and of a receptor that mediates the stimulation of macrophages were decreased significantly (see *Bst2* and *Mst1r* in Table 3). The data suggest that formation of immune tolerance or immune defense in response to infections may the disturbed after HFD.

Effect of HFD on Proteins Involved in Inflammation

Crohn's disease (CD) is a relatively frequent inflammation diseases in the small intestine. It has a similar etiology to colitis ulcerosa[26,27] and mucositis after treatment with cytostatics such as 5-fluorouracil.[28] Since the inflammatory bowel diseases CD and colitis ulcerosa are characterized by a dysregulated immune response to bacteria in the gut, the observed down-regulation of proteins involved in immune tolerance and immune defense after HFD may have an impact on CD. CD was associated with mutations in several genes.[26,27] Expression levels of four of these genes (Atg16l1, Stat3, Nkx2−3, *Irgm*) were detected in our preparation; however, the expression levels were not changed significantly after HFD (Table 8, Supporting Information). We also detected several components of the transcriptional regulator NF-kappa B, which plays a central role in signaling during intestinal mucositis.[28] Also the expression levels of these genes were not changed significantly (Table 4, Supporting Information). After HFD, three proinflammatory genes were significantly down-regulated (see *Ctnnb1*, *Itgal*, *Itgb2* in Table 7, Supporting Information). Catenin beta (*Ctnnb1*) activates proinflammatory signaling pathways, whereas integrin alpha l (*Itgal*) and integrin beta 2 (*Itgb2*) mediate leukocyte adhesion during inflammation (Table 8, Supporting Information). Functional studies are required to determine whether these changes in expression are functionally relevant for CD or drug-induced mucositis.

DISCUSSION

By using recently improved methods for analysis and quantification of proteins in biological samples, more than 5000 different proteins were quantified in lysates of small intestinal mucosa from mice that were fed for two months with ND or HFD. The obtained data provide a comprehensive overview about the expression levels of genes in the small intestine. This information is important for the understanding of the physiological significance of individual proteins in the small intestine. For example, our data show that the expression level of the Na^+-D-glucose cotransporter SGLT1 (gene *Slc5a1*) is 42-times higher than expression of the most strongly expressed subtype of the Na^+-proton exchanger NHE3 (gene *Slc9a3*) (Table 5, Supporting Information). Concerning polyspecific drug transporters in the BBM of enterocytes, they show that the ATP-dependent efflux pumps MDR1a (gene *Abcb1a*) and BCRP (gene *Abcg2*) and the proton-peptide cotransporter PEPT1 (gene *Slc15a1*), which transports for example lactam antibiotics into cells, are most strongly expressed, whereas the expression level of the polyspecific organic cation transporter OCT1 in the BBM (gene *Slc22a1*) is 4−8 times lower.[29,30] Organic cation transporter OCT3, which was assumed to be also expressed in the BBM, was not detected in our preparations. Another remarkable observation is the high expression of MHCII components (genes *H2A-a*, *H2A-b1*, *H2E-b1*). The MHCII is involved in the formation of immune tolerance and associated with tolerosomes.[24]

Since the mucosal scrapings analyzed in our study represent mainly proteins from enterocytes but also contain proteins of the underlying connective tissue, the interpretation of the data must be performed in context with current knowledge concerning cellular and subcellular locations of the proteins. Solely on the basis of our data it cannot be distinguished whether cellular proteins with low expression are derived from enterocytes, secretory cells within the epithelial lining, or from cells within the underlying connective tissue. To determine protein expression levels within individual cell types and within their subcellular compartments, highly efficient purification procedures are required. This is a serious bottleneck and remains a challenge for future proteomic analyses. For example, the previously reported proteomic analyses of BBM preparations from mouse small intestine revealed large fractions of

mitochondrial and nuclear proteins,[4,5] which indicates that the analyzed BBM preparations were impure. In this work, we made the attempt to characterize the proteome of cellular membranes and tried to obtain more defined information about the expression of nutrient transporters. Unfortunately, we failed to obtain membrane fractions that were substantially depleted from mitochondria and other organelles; however, the proteomic analysis allowed the quantitative analysis of additional membrane proteins.

The small intestine represents a large surface for the first contact of ingested food, drugs, xenobiotics, bacteria, and viruses. Thus, it would make physiological sense if the expression of uptake systems for nutrients and drugs as well as the expression of metabolizing enzymes would be regulated in response to diets or oral consumption of drugs. Diet-dependent regulation was reported for some transporters. For example, it was described that the expression of the Na^+-D-glucose cotransporter SGLT1 (gene *Slc5a1*) in small intestine is regulated in response to the glucose content of the diet[31] and that the expression of Na^+-phosphate transporter NaPi IIb (gene *Sl34a2*) is in response to phosphate in the diet.[32] So far no overview concerning the effects of different diets on the expression of small intestinal proteins were available. To test whether the optimized quantitative proteome analysis is appropriate to obtain such information, we investigated the effect of HFD. This diet containing a high content of fat and monosaccharides was selected because it is similar to the Western diet and overnutrition; this type of food is the main reason for obesity in industrial countries. Obesity is a main risk factor for type 2 diabetes (T2D) and many other diseases.[33,34] The pathophysiological mechanism of how overnutrition-induced obesity promotes T2D was investigated using mice that were fed with HFDs including the HFD used in our study.[15,35] By focusing on changes subsequent to obesity, the pathophysiological mechanism for the development of T2D was attributed to secretion of fat-derived incretins leading to increased insulin secretion, decreased insulin receptor sensitivity, proliferation of pancreatic beta cells, and finally destruction of the beta cells. It was shown that the development of T2D is accelerated by inflammation.[36] We wondered whether HFD influences the protein composition of small intestinal mucosa and gives a hint at functional changes with impact on the development or promotion of T2D.

After two months of HFD, distinct changes in the expression of proteins in the small intestinal mucosa were observed. Notwithstanding that changed protein concentrations cannot be directly correlated with changed functions, the obtained changes strongly suggest altered absorption of nutrients and drugs and altered metabolism of nutrients and drugs within small intestine as well as altered immune tolerance and immune defense. After HFD, proteins involved in transmembrane uptake of FAs (see FATP2 in Table 1), intracellular FA translocation (Figure 4A and Figure 2F), basolateral export of chylomicrons (Figure 2F), mitochondrial FA β-oxidation (Figure 4B), triglyceride synthesis (Figure 4D), and steroid metabolism (Figure 4E,F) were increased. The increased expression of components of protein complexes that are involved in transcription, RNA processing, and protein translation (Figure 2D) may be due to a high demand for lipid packing proteins. By anticipating up-regulation of proteins involved in lipid handling in response to lipid overload, the observed changes may have been expected. A more surprising observation was that the expression of several transporters that mediate nutrient absorption was decreased (Table 1). Importantly, the Na^+-D-glucose cotransporter SGLT1 in the BBM, which is rate limiting for glucose absorption, and the glucose facilitator GLUT2, which mediates the release of glucose,[16] were decreased by 60−70%. This suggests that the glucose absorption is slowed down after HFD. This interpretation is supported by our observation that the SGLT1-mediated uptake of glucose into enterocytes was decreased by 20%. The observed down-regulation of the Na,K-ATPase may be explained as a consequence of a reduced intracellular Na^+ load because of the down-regulation of SGLT1 and some other Na^+-cotransporters in the BBM. The down-regulation of glucose uptake into enterocytes after HFD is consistent with the decreased expression of most enzymes involved in glycolysis, the pyruvate dehydrogenase complex, and the Krebs cycle (Figure 3A,E,F). This suggests a decrease of the catabolic glucose metabolism; however, because of increased lipid catabolism (Figure 4B,E,F), the total energy generation appears to be increased after HFD as suggested by the increased expression of components of the respiratory chain (Figure 3G) and the mitochondrial ATP synthase (see gene *Atp1a1* in Table 2, Supporting Information).

Our data suggest that the small intestinal absorption of many drugs and xenobiotics as well as the first-pass metabolism of drugs and xenobiotics in the intestine is changed after HFD. The permeation of lipophilic drugs and xenobiotics across the BBM of the enterocytes is limited by ATP-dependent export pumps such as MDR1a and breast-cancer related protein (BCRP), whereas the uptake of hydrophilic drugs is mediated by transporters such as PEPT1 and OCT1. In addition to transporters, the pharmacokinetics of drugs is influenced by the metabolizing and modifying intracellular enzymes.[2,20,37] Since the expression of BCRP was decreased by 67% after HFD, the uptake of drugs translocated by BCRP into the enterocytes such as the cytostatic tropotecan, antidiabetic glyburide, antibiotic nitrofurantoin, and cholesterol-lowering statins should be increased.[38,39] Whether this leads to increased small intestinal absorptions and changed pharmacokinetics depends on the metabolism and modification of the individual drugs in the small intestine as well as the utilized export pathway across the BLM. After HFD, oral absorption of drugs such as doxorubicin, which is transported by both MDR1 in the BBM and by MRP3 in the BLM,[40,41] may be decreased since the expression of MRP3 was decreased, whereas the expression of MDR1 was not changed. The potential relevance of the observed HFD-induced changes of metabolic enzymes may be demonstrated by two examples. The observed down-regulation of three strongly expressed carboxyesterases (Table 2 genes *Ces2g*, *Ces2e*, and *Ces3*) suggests that the degradation of drugs that are inactivated by decarboxylation such as the antihypertensive delapril is decreased after HFD.[42] On the other hand, prodrugs that are activated by decarboxylation, for example, the antitumor drug CPT-11, which is used for treatment of colon cancer, may be activated more slowly to the active compound SN38.[42] Since delayed diarrhea is a dose-limiting side effect of SN38, a HFD may help. An interesting observation was that the most strongly expressed alcohol dehydrogenase ADH-1, which is rate-limiting for alcohol metabolism and expressed in the enterocytes,[43] was up-regulated 3.4-fold after HFD (Table 2). This suggests that first-pass metabolism of ethanol in the small intestine is accelerated, and ethanol tolerance may be increased after HFD.

dx.doi.org/10.1021/pr500833v | J. Proteome Res. 2015, 14, 353−365

After two months of HFD, no changes of expression of inflammation-related genes were observed, which indicates that the HFD did not lead to inflammation; however, since components of IgG, IgA, and IgM were down-regulated, the susceptibility to bacterial or viral infections may be increased. On the basis of the observed down-regulation of components of the MHCII by HFD, it may be speculated that HFD has effects on the generation, progression, or therapeutic outcome of Crohn's disease. Inflammation models in mice may be employed for evaluation.

The observed effects of HFD on the expression of physiological relevant proteins gave rise to various hypotheses concerning beneficial or negative effects of this diet. For example, HFD may alter the absorption of nutrients and drugs, pharmacokinetics and toxicity of drugs, immunological defense against bacterial infection, and immunotolerance. Considering the limitation of a purely proteomic analysis concerning functional interpretations, experimental testing of the individual mucosal functions and metabolic pathways is required to allow defined conclusions concerning functional effects of HFD. Future proteomic analyses may clarify whether the carbohydrates in the employed HFD are essential for the observed effects on protein expression and whether feeding for two months is necessary to induce the observed changes or if a shorter feeding period is sufficient. It is also important to determine the cellular and intracellular location of the proteins with different expression to distinguish between transcriptional/translational and posttranslational effects of HFD.

■ ASSOCIATED CONTENT

Supporting Information

Figure of glycan biosynthesis. Tables of complete spectra search output and unprocessed MaxQuant output; LFQ and TPA protein quantitation of whole lysates; principal component analysis; quantitation of proteins identified in membrane fractions; quantified plasma membrane transporters in mouse small intestinal mucosa after ND; supplemental table to Figure 2, content of subcellular fractions and groups of proteins; concentrations of drug metabolizing enzymes in mouse small intestinal mucosa after ND; and expression of proteins involved in antibody mediated immune reactions (AMIR) that may be responsible for immune defense or immune tolerance, innate immunity (IIM), defense against bacteria, viruses, and parasites (BVPD) and inflammation (IF). This material is available free of charge via the Internet at http://pubs.acs.org.

■ AUTHOR INFORMATION

Corresponding Author

*E-mail: jwisniew@biochem.mpg.de. Phone: 49 89 85782205. Fax: 49 89 85782219.

Notes

The authors declare no competing financial interest.

■ ACKNOWLEDGMENTS

We thank Katharina Zettl for the excellent technical assistance and Korbinian Mayr for the support in mass spectrometric analysis. This work was supported by the Max−Planck Society for the Advancement of Science and the Deutsche Forschungsgemeinschaft (Grant No. KO 872/5-1).

■ ABBREVIATIONS

BLM, basolateral membrane; BBM, BBM; ND, normal diet; HFD, high-fat diet; WCL, whole cell lysate; ML, membrane lysate; PBS, phosphate buffered saline; FASP, filter-aided sample preparation; MED, multienzyme digestion; SAX, strong anion exchange separation; LC−MS/MS, liquid chromatography tandem spectrometry; HCD, high energy collisional dissociation; LFQ, label free quantification; TPA, total protein approach; AMG, α-methyl D-glucopyranoside; FA, fatty acid; TG, triglyceride; PCA, principal component analysis; MHC, major histocompatibility complex; CD, Crohn's disease; T2D, type 2 diabetes

■ REFERENCES

(1) Koepsell, H. The SLC22 family with transporters of organic cations, anions, and zwitterions. *Mol. Aspects Med.* **2013**, *34*, 413−435.
(2) Suzuki, H.; Sugiyama, Y. Role of metabolic enzymes and efflux transporters in the absorption of drugs from the small intestine. *Eur. J. Pharm. Sci.* **2000**, *12*, 3−12.
(3) Kaminsky, L. S.; Zhang, Q. Y. The small intestine as a xenobiotic-metabolizing organ. *Drug Metab. Dispos.* **2003**, *31*, 1520−1525.
(4) McConnell, R. E.; Benesh, A. E.; Mao, S.; Tabb, D. L.; Tyska, M. J. Proteomic analysis of the enterocyte brush border. *Am. J. Physiol.: Gastrointest. Liver Physiol.* **2011**, *300*, G914−G926.
(5) Donowitz, M.; Singh, S.; Salahuddin, F. F.; Hogema, B. M.; Chen, Y.; Gucek, M.; Cole, R. N.; Ham, A.; Zachos, N. C.; Kovbasnjuk, O.; Lapierre, L. A.; Broere, N.; Goldenring, J.; deJonge, H.; Li, X. Proteome of murine jejunal brush border membrane vesicles. *J. Proteome Res.* **2007**, *6*, 4068−4079.
(6) Wisniewski, J. R.; Zougman, A.; Nagaraj, N.; Mann, M. Universal sample preparation method for proteome analysis. *Nat. Methods* **2009**, *6*, 359−362.
(7) Cox, J.; Mann, M. MaxQuant enables high peptide identification rates, individualized p.p.b.-range mass accuracies, and proteome-wide protein quantification. *Nat. Biotechnol.* **2008**, *26*, 1367−1372.
(8) Wisniewski, J. R.; Mann, M. Consecutive proteolytic digestion in an enzyme reactor increases depth of proteomic and phosphoproteomic analysis. *Anal. Chem.* **2012**, *84*, 2631−2637.
(9) Wisniewski, J. R.; Zielinska, D. F.; Mann, M. Comparison of ultrafiltration units for proteomic and *N*-glycoproteomic analysis by the filter-aided sample preparation method. *Anal. Biochem.* **2011**, *410*, 307−309.
(10) Wisniewski, J. R.; Zougman, A.; Mann, M. Combination of FASP and StageTip-based fractionation allows in-depth analysis of the hippocampal membrane proteome. *J. Proteome Res.* **2009**, *8*, 5674−5678.
(11) Olsen, J. V.; Macek, B.; Lange, O.; Makarov, A.; Horning, S.; Mann, M. Higher-energy C-trap dissociation for peptide modification analysis. *Nat. Methods* **2007**, *4*, 709−712.
(12) Cox, J.; Neuhauser, N.; Michalski, A.; Scheltema, R. A.; Olsen, J. V.; Mann, M. Andromeda: A peptide search engine integrated into the MaxQuant environment. *J. Proteome Res.* **2011**, *10*, 1794−1805.
(13) Benjamini, Y.; Hochberg, Y. Controlling the false discovery rate: A practical and powerful approach to multiple testing. *J. R. Stat. Soc.* **1995**, *57*, 289−300.
(14) Wisniewski, J. R.; Ostasiewicz, P.; Dus, K.; Zielinska, D. F.; Gnad, F.; Mann, M. Extensive quantitative remodeling of the proteome between normal colon tissue and adenocarcinoma. *Mol. Syst. Biol.* **2012**, *8*, 611.
(15) Benhamed, F.; Denechaud, P. D.; Lemoine, M.; Robichon, C.; Moldes, M.; Bertrand-Michel, J.; Ratziu, V.; Serfaty, L.; Housset, C.; Capeau, J.; Girard, J.; Guillou, H.; Postic, C. The lipogenic transcription factor ChREBP dissociates hepatic steatosis from insulin resistance in mice and humans. *J. Clin. Invest.* **2012**, *122*, 2176−2194.
(16) Gorboulev, V.; Schürmann, A.; Vallon, V.; Kipp, H.; Jaschke, A.; Klessen, D.; Friedrich, A.; Scherneck, S.; Rieg, T.; Cunard, R.; Veyhl-Wichmann, M.; Srinivasan, A.; Balen, D.; Breljak, D.; Rexhepaj, R.;

Parker, H. E.; Gribble, F. M.; Reimann, F.; Lang, F.; Wiese, S.; Sabolic, I.; Sendtner, M.; Koepsell, H. Na+-D-glucose cotransporter SGLT1 is pivotal for intestinal glucose absorption and glucose-dependent incretin secretion. *Diabetes* **2012**, *61*, 187−196.
(17) Anderson, C. M.; Stahl, A. SLC27 fatty acid transport proteins. *Mol. Aspects Med.* **2013**, *34*, 516−528.
(18) Traiffort, E.; O'Regan, S.; Ruat, M. The choline transporter-like family SLC44: Properties and roles in human diseases. *Mol. Aspects Med.* **2013**, *34*, 646−654.
(19) Koepsell, H.; Lips, K.; Volk, C. Polyspecific organic cation transporters: Structure, function, physiological roles, and biopharmaceutical implications. *Pharm. Res.* **2007**, *24*, 1227−1251.
(20) Benet, L. Z.; Cummins, C. L. The drug efflux−metabolism alliance: Biochemical aspects. *Adv. Drug Delivery Rev.* **2001**, *50* (Suppl. 1), S3−S11.
(21) Ding, X.; Kaminsky, L. S. Human extrahepatic cytochromes P450: Function in xenobiotic metabolism and tissue-selective chemical toxicity in the respiratory and gastrointestinal tracts. *Annu. Rev. Pharmacol. Toxicol.* **2003**, *43*, 149−173.
(22) Paine, M. F.; Hart, H. L.; Ludington, S. S.; Haining, R. L.; Rettie, A. E.; Zeldin, D. C. The human intestinal cytochrome P450 "pie". *Drug Metab. Dispos.* **2006**, *34*, 880−886.
(23) Miron, N.; Cristea, V. Enterocytes: Active cells in tolerance to food and microbial antigens in the gut. *Clin. Exp. Immunol.* **2012**, *167*, 405−412.
(24) Ostman, S.; Taube, M.; Telemo, E. Tolerosome-induced oral tolerance is MHC-dependent. *Immunology* **2005**, *116*, 464−476.
(25) Hansen, G. H.; Niels-Christiansen, L. L.; Immerdal, L.; Danielsen, E. M. Antibodies in the small intestine: Mucosal synthesis and deposition of anti-glycosyl IgA, IgM, and IgG in the enterocyte brush border. *Am. J. Physiol.: Gastrointest. Liver Physiol.* **2006**, *291*, G82−G90.
(26) Baumgart, D. C.; Carding, S. R. Inflammatory bowel disease: Cause and immunobiology. *Lancet* **2007**, *369*, 1627−1640.
(27) Xavier, R. J.; Podolsky, D. K. Unravelling the pathogenesis of inflammatory bowel disease. *Nature* **2007**, *448*, 427−434.
(28) Chang, C. T.; Ho, T. Y.; Lin, H.; Liang, J. A.; Huang, H. C.; Li, C. C.; Lo, H. Y.; Wu, S. L.; Huang, Y. F.; Hsiang, C. Y. 5-Fluorouracil-induced intestinal mucositis via nuclear factor-kappaB activation by transcriptomic analysis and in vivo bioluminescence imaging. *PLoS One* **2012**, *7*, e31808.
(29) Han, T. K.; Everett, R. S.; Proctor, W. R.; Ng, C. M.; Costales, C. L.; Brouwer, K. L.; Thakker, D. R. Organic cation transporter 1 (OCT1/mOct1) is localized in the apical membrane of Caco-2 cell monolayers and enterocytes. *Mol. Pharmacol.* **2013**, *84*, 182−189.
(30) Shugarts, S.; Benet, L. Z. The role of transporters in the pharmacokinetics of orally administered drugs. *Pharm. Res.* **2009**, *26*, 2039−2054.
(31) Ferraris, R. P.; Diamond, J. M. Specific regulation of intestinal nutrient transporters by their dietary substrates. *Annu. Rev. Physiol.* **1989**, *51*, 125−141.
(32) Forster, I. C.; Hernando, N.; Biber, J.; Murer, H. Phosphate transporters of the SLC20 and SLC34 families. *Mol. Aspects Med.* **2013**, *34*, 386−395.
(33) Wild, S.; Roglic, G.; Green, A.; Sicree, R.; King, H. Global prevalence of diabetes: Estimates for the year 2000 and projections for 2030. *Diabetes Care* **2004**, *27*, 1047−1053.
(34) Guh, D. P.; Zhang, W.; Bansback, N.; Amarsi, Z.; Birmingham, C. L.; Anis, A. H. The incidence of comorbidities related to obesity and overweight: A systematic review and meta-analysis. *BMC Public Health* **2009**, *9*, 88.
(35) Winzell, M. S.; Ahren, B. The high-fat diet-fed mouse: A model for studying mechanisms and treatment of impaired glucose tolerance and type 2 diabetes. *Diabetes* **2004**, *53* (Suppl. 3), S215−S219.
(36) Ding, S.; Chi, M. M.; Scull, B. P.; Rigby, R.; Schwerbrock, N. M.; Magness, S.; Jobin, C.; Lund, P. K. High-fat diet: Bacteria interactions promote intestinal inflammation, which precedes and correlates with obesity and insulin resistance in mouse. *PLoS One* **2010**, *5*, e12191.
(37) Paine, M. F.; Shen, D. D.; Kunze, K. L.; Perkins, J. D.; Marsh, C. L.; McVicar, J. P.; Barr, D. M.; Gillies, B. S.; Thummel, K. E. First-pass metabolism of midazolam by the human intestine. *Clin. Pharmacol. Ther.* **1996**, *60*, 14−24.
(38) Kruijtzer, C. M.; Beijnen, J. H.; Rosing, H.; ten Bokkel Huinink, W. W.; Schot, M.; Jewell, R. C.; Paul, E. M.; Schellens, J. H. Increased oral bioavailability of topotecan in combination with the breast cancer resistance protein and *P*-glycoprotein inhibitor GF120918. *J. Clin. Oncol.* **2002**, *20*, 2943−2950.
(39) Ni, Z.; Bikadi, Z.; Rosenberg, M. F.; Mao, Q. Structure and function of the human breast cancer resistance protein (BCRP/ABCG2). *Curr. Drug Metab.* **2010**, *11*, 603−617.
(40) Young, L. C.; Campling, B. G.; Voskoglou-Nomikos, T.; Cole, S. P.; Deeley, R. G.; Gerlach, J. H. Expression of multidrug resistance protein-related genes in lung cancer: Correlation with drug response. *Clin. Cancer Res.* **1999**, *5*, 673−680.
(41) van der Sandt, I. C.; Blom-Roosemalen, M. C.; de Boer, A. G.; Breimer, D. D. Specificity of doxorubicin versus rhodamine-123 in assessing *P*-glycoprotein functionality in the LLC-PK1, LLC-PK1:MDR1, and Caco-2 cell lines. *Eur. J. Pharm. Sci.* **2000**, *11*, 207−214.
(42) Redinbo, M. R.; Potter, P. M. Mammalian carboxylesterases: From drug targets to protein therapeutics. *Drug Discovery Today* **2005**, *10*, 313−325.
(43) Haselbeck, R. J.; Duester, G. Regional restriction of alcohol/retinol dehydrogenases along the mouse gastrointestinal epithelium. *Alcohol.: Clin. Exp. Res.* **1997**, *21*, 1484−1490.